Imaging Patterns in Occupational Lung Disease—When Should I Consider?

Yasmeen K. Tandon, MD, Lara Walkoff, MD*

KEYWORDS

• Pneumoconiosis • Occupational lung disease • Inhalational lung disease

KEY POINTS

- Despite workplace safety regulations, occupational lung diseases (OLDs) remain a leading cause of work-related illnesses.
- Substantial overlap exists between the imaging appearance of many OLDs and other entities; therefore, an OLD should be considered when formulating a differential.
- Diagnosing OLDs often requires a multidisciplinary approach, which includes a detailed clinical history, imaging findings, and sometimes histopathology.

INTRODUCTION

Occupational lung diseases (OLDs) encompass a broad group of entities related to workplace exposures that result from the inhalation of organic or inorganic antigens.[1] Pneumoconioses are a subgroup of OLDs caused by the inhalation of inorganic mineral dusts. Despite safety regulations, OLDs remain a leading cause of work-related illness and mortality.[2] Manifestations of OLDs depend on the properties of the inhaled substance, intensity and duration of exposure, and the susceptibility of an individual.[3,4]

Diagnosing OLDs can be challenging due to the absence of an exposure history, potentially long latency between exposure and manifestation, entities unrelated to occupational exposures producing similar imaging findings, single agents resulting in variety of manifestations, and some OLDs that can result from multiple different inhaled antigens.[4] Additionally, symptoms are often nonspecific and may not occur until late in the course of the disease.[5] Establishing the correct diagnosis often requires a multidisciplinary approach and depends on the integration of a thorough exposure history, laboratory results, diagnostic imaging, pulmonary function testing, and sometimes biopsy.[5] Because imaging plays such a key role in diagnosis, it is imperative that radiologists consider OLDs in the differential and remain apprised of evolving industrial practices.

IMAGING TECHNIQUE

Imaging is central in the diagnosis and monitoring of OLDs. Because chest radiographs are widely available, inexpensive, and relatively low radiation dose, they remain the primary imaging modality for both the initial evaluation of suspected OLDs and occupational exposure surveillance programs.[6] However, numerous studies have shown radiographs to be both less sensitive and less specific than CT for the detection and characterization of many OLDs.[7–10] The International Labor Organization (ILO) has a standardized classification system based on the posteroanterior (PA) chest radiograph evaluating multiple subcategories of pleural and parenchymal abnormalities to codify changes related to pneumoconioses for epidemiologic research, screening, surveillance, and clinical

Mayo Clinic Department of Radiology, 200 First Street Southwest, Rochester, MN 55905, USA
* Corresponding author.
E-mail address: Walkoff.Lara@mayo.edu

Radiol Clin N Am 60 (2022) 979–992
https://doi.org/10.1016/j.rcl.2022.06.011
0033-8389/22/

Abbreviations	
CWP	coal worker's pneumoconiosis
NSIP	nonspecific interstitial pneumonia
UIP	usual interstitial pneumonial
PF	idiopathic pulmonary fibrosis

purposes, although no diagnosis is assigned.[11] High-resolution computed tomography (HRCT) is primarily is used to characterize abnormalities identified on radiographs, evaluate equivocal radiographs, and assess symptomatic patients.[6] (18)F-fluorodeoxyglucose (FDG) PET and MR imaging are not routinely used for screening or surveillance of OLDs, however may have utility in specific situations, such as in the evaluation of associated bronchogenic malignancies or mesothelioma.

IMAGING PROTOCOLS

When radiographs are used for the evaluation for OLDs 2 views, both PA and lateral, should be obtained, if possible. A HRCT protocol for the evaluation of OLDs should include thin-section noncontrast supine inspiratory views, expiratory imaging to evaluate for air trapping, and prone imaging to differentiate dependent atelectasis from fibrosis.

IMAGING FINDINGS

The most common HRCT patterns associated with various OLDs are summarized in **Table 1**.

ASBESTOS

Inhalation of asbestos fibers occurs in occupations such as asbestos mining, asbestos abatement, or industries such as ship building, brake manufacturing, insulation, and construction.[4] Pathogenesis depends on asbestos fiber shape and size, fiber dose, duration of exposure, concurrent exposures, and host immune factors.[12] Both pulmonary parenchymal and pleural manifestations of asbestos exposure tend to have long latency periods on the order of decades.

Asbestos-Related Pleural Disease

Benign asbestos-related pleural effusions are typically the earliest asbestos-related pleural change with onset as early as 10 years exposure; however, they are less common than pleural plaques.[13,14] The effusions are usually small, exudative (may be hemorrhagic), can be unilateral or bilateral, and can persist, resolve, and/or recur over

Table 1
Typical thoracic high-resolution computed tomography patterns in occupational lung diseases

Pulmonary parenchyma	
Fibrosis	Aluminosis[56] Asbestosis[24] CBD[46] Chronic HP[61] Chronic silicosis[31] CWP[31] HMP[52] Inhalational talcosis[35]
Centrilobular nodules	Acute silicosis[33] Aluminosis[56] Chronic silicosis[35] CWP[35] Inhalational talcosis[49] Siderosis[51] Subacute HP[61]
Perilymphatic nodules	CBD[46] Chronic silicosis[35] CWP[35]
Consolidative opacities	Acute HP[3] Acute silicosis[33] HMP[52]
GGOs	Acute silicosis[33] CBD[46] HMP[52] Subacute or chronic HP[61,63]
Conglomerate masses	CBD[46] Complicated silicosis[31] Complicated CWP[31] Inhalational talcosis[50]
Rounded atelectasis	Asbestos exposure[27]
Cysts	Chronic HP[63]
Air trapping	Subacute or chronic HP[61,63] Work-related asthma[6]
Pleura	
Effusion	Asbestos exposure[13]
Thickening	Asbestos exposure[13]
Plaques	Asbestos exposure[13] CBD (pseudoplaques)[45] Chronic silicosis (pseudoplaques)[4] CWP (pseudoplaques)[4] Inhalational talcosis[49]
Other	
Calcified lymph nodes	CBD[39] Chronic silicosis[31] Chronic CWP[31]

time.[14,15] In the absence of other imaging findings of prior asbestos exposure, the appearance mimics other causes of exudative effusions including infection and malignancy. Mesothelioma should be considered in cases of late developing or recurrent pleural effusions.[13]

Diffuse pleural thickening (DPT) is due to thickening of the visceral pleura[11] and most commonly involves the posterior and posteromedial pleura over the lower lobes.[16] DPT is a less specific indicator of prior asbestos exposure than pleural plaques and can also occur in the setting of prior infection, hemothorax, and connective tissue disease.[13] Unlike pleural plaques, DPT rarely calcifies, although it may coexist with calcified pleural plaques (CPP; **Fig. 1**).[17] Some variation in the definition of DPT exists; however, McLoud and colleagues defined DPT on chest radiography as "a smooth, non-interrupted pleural density extending over at least one-fourth of the chest wall, with or without costophrenic angle obliteration,"[18] although the ILO definition must include an obliterated costophrenic angle.[11] On CT, DPT has been defined by Lynch and colleagues as "a continuous sheet of pleural thickening more than 5 cm wide, more than 8 cm in craniocaudal extent, and more them 3 mm thick."[16] In contrast to well-circumscribed pleural plaques, the margin between the DPT and adjacent lung is commonly irregular due to underlying fibrosis.[19]

Asbestos-related pleural plaques, focal protrusions of hyaline fibrosis arising from the parietal pleura that often calcify, are the most common manifestation of prior asbestos exposure.[13] Plaques are typically not detected radiographically until at least 20 years after exposure.[17] Pleural plaques commonly involve the hemidiaphragms (virtually pathognomonic), with other characteristic locations including the mid to lower posterior and posterolateral chest wall, paravertebral pleura, and sometimes the mediastinal pleura. Asbestos-related pleural plaques rarely involve the apices or costophrenic sulci, unlike DPT.[17] Plaques are usually present bilaterally but may have an asymmetric distribution. On frontal radiographs, pleural plaques can appear as a focal opacity projected over the lung when present along the anterior and posterior chest wall and viewed en face. A high attenuation, serpentine, peripheral margin of calcification may be visible, resembling a holly leaf.[20] When viewed in profile the plaques have a more linear configuration (**Fig. 2**). Subpleural fat,

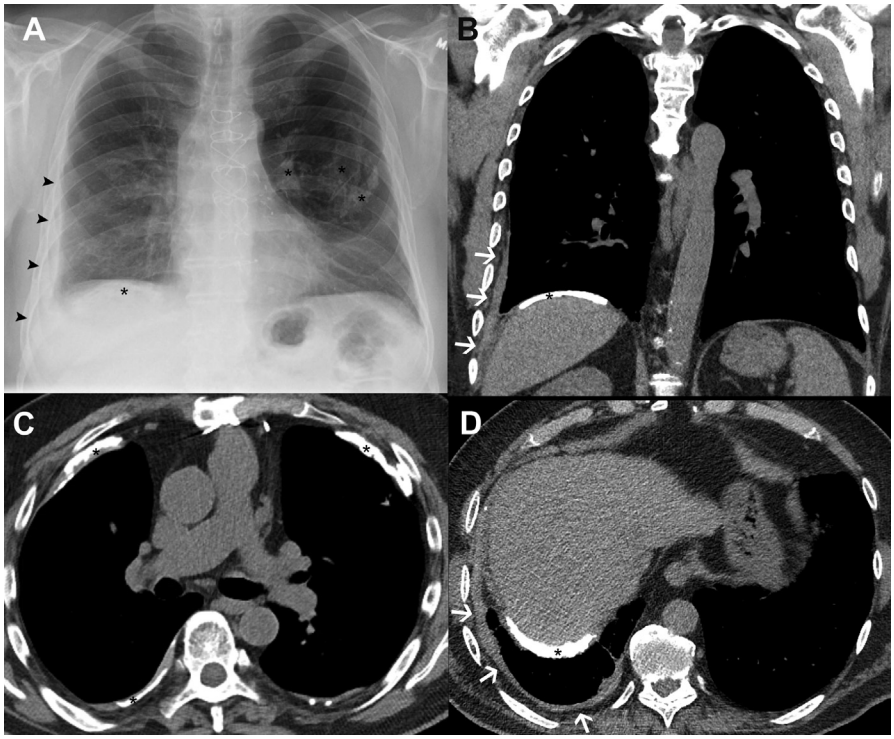

Fig. 1. DPT and pleural plaques. Frontal chest radiograph (*A*) demonstrates CPP bilaterally (*) and smooth linear opacity, DPT, along the inferior third of the right hemithorax extending into the lateral costophrenic sulcus (*arrowheads*). Coronal (*B*) and axial (*C*, *D*) CT images demonstrate DPT in this patient with prior asbestos exposure (*arrows*, *B* and *D*). CPP are also present bilaterally (*).

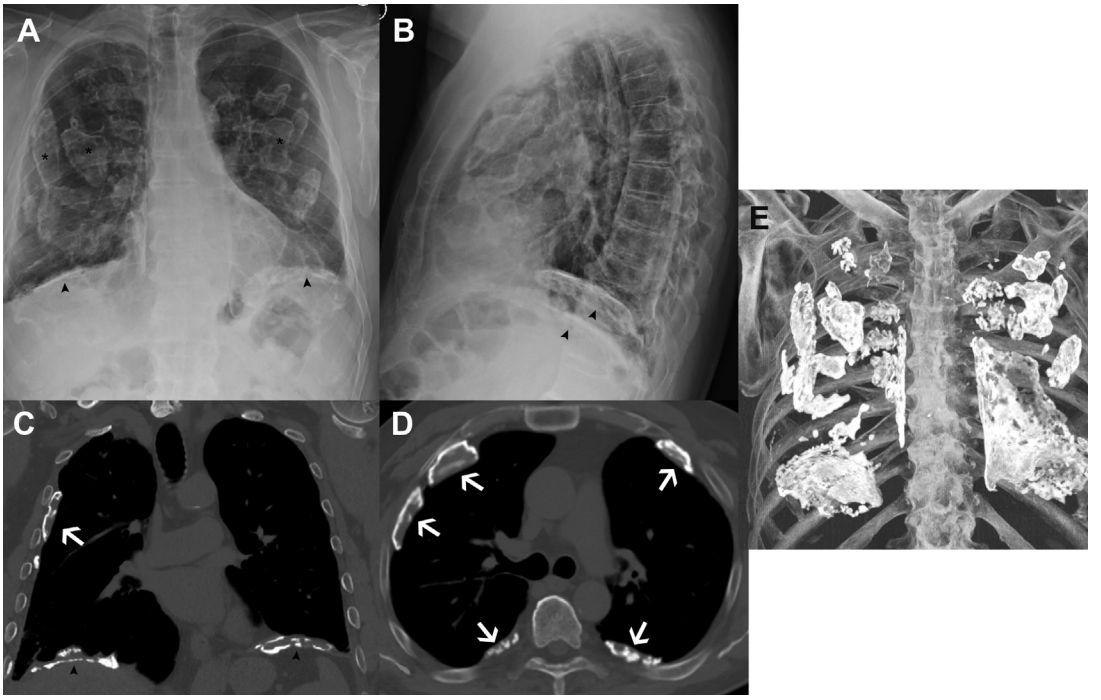

Fig. 2. CPP due to asbestos exposure. Frontal (*A*) and lateral (*B*) chest radiographs with extensive CPP visible en face along the chest wall (eg, * in *A*). CPP are also present along both hemidiaphragms, (*arrowheads*). Coronal (*C*) and axial (*D*) CT images show partially calcified plaques along the chest wall (*arrows*) and hemidiaphragms (*arrowheads*). Coronal 3D MIP rendering (*E*) shows the extent and distribution of the plaques.

rib fractures, and companion shadows from chest wall musculature can mimic pleural plaques on frontal radiograph.[17] On CT, pleural plaques are focal circumscribed areas of pleural thickening separated from the underlying ribs and other extrapleural structures by a thin layer of fat. Punctate, linear, or coalescent calcification may be present.[19] CT is more sensitive than radiograph for the detection of both pleural plaques and DPT.[9]

Malignant Pleural Mesothelioma

Asbestos is a known carcinogen, which increases the risk of malignant pleural mesothelioma (MPM; as well as bronchogenic malignancies), with the most MPM cases related to prior asbestos exposure.[21] MPM is typically not diagnosed until 20 to 40 years after exposure.[3] Pleural thickening and pleural effusions are common (**Fig. 3**). CT features that are more often present in MPM compared with benign pleural disease such as DPT include mediastinal pleural thickening, pleural rind, pleural nodularity, and parietal pleural thickening measuring more than 1 cm in thickness.[22]

Parenchymal

Asbestosis is diffuse pulmonary fibrosis, which typically occurs in individuals with prolonged and high concentration exposure to asbestos fibers. A dose-dependent relationship between exposure and fibrosis exists. Asbestosis usually occurs 20 years or greater after exposure.[3] Radiographs show small bilateral reticular opacities with a lower lung and peripheral predominance, which become more diffuse and as fibrosis progresses. The earliest HRCT manifestation of asbestosis is small, round, branching subpleural centrilobular opacities reflecting fibrosis in the walls of the respiratory bronchiole.[23] Typical HRCT findings include intralobular lines, interlobular septal thickening, ground glass opacities (GGOs), subpleural curvilinear opacities, and parenchymal bands (**Fig. 4**). Subpleural curvilinear opacities are linear densities paralleling the inner chest wall located within 1 cm of the pleura. Parenchymal bands are linear densities measuring 2 to 5 cm in length coursing through the lung to contact the pleural surface, often associated with parenchymal distortion, which do not resolve on prone imaging.[24] Subpleural curvilinear opacities and parenchymal bands are not specific for asbestosis, although have been observed more commonly in asbestosis than in some other causes of fibrosing pneumonia.[25] Honeycombing may occur in advanced disease. IPF and other causes of a UIP pattern can have similar manifestations. However,

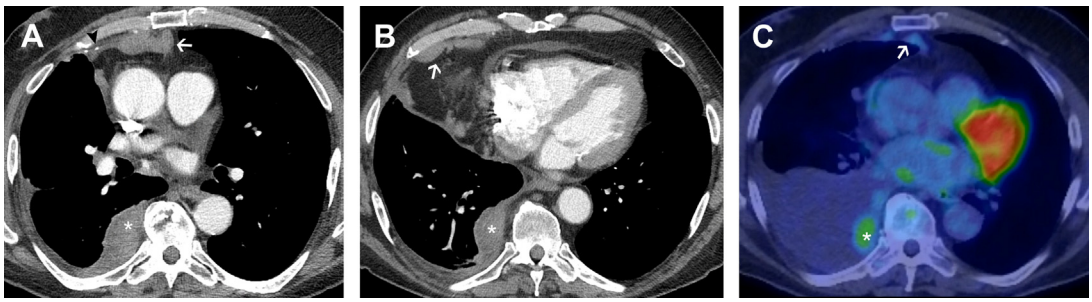

Fig. 3. MPM (epithelioid). Axial CT images (*A*, *B*) and axial FDG PET/CT fusion image (*C*) showing lobulated soft tissue masses along the right posteromedial pleural space with increased FDG activity (*). Enlarged and mildly FDG avid right cardiophrenic angle lymph nodes are also present (*arrows*). Note a small CPP (*arrowhead*, *A*) compatible with history of prior asbestos exposure. Note the accumulation of right pleural fluid between the CT and PET/CT performed 3 months apart.

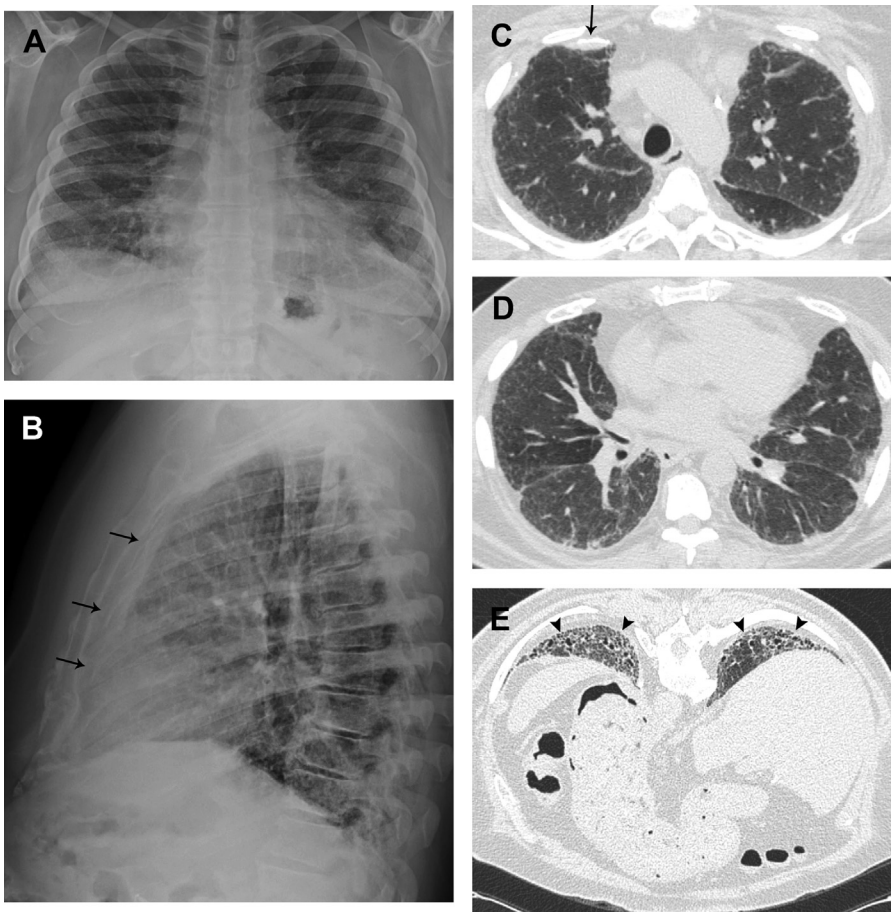

Fig. 4. Asbestosis. PA (*A*) and lateral (*B*) chest radiograph images demonstrate lower lung zone predominant fine reticular opacities and partially CPP (*arrow*, *B*). Axial CT images from the upper (*C*), mid (*D*), and lower (*E*) lungs also show lower lung predominant reticulations with associated ground glass and traction bronchiectasis (*arrowheads*, *E*). Note persistence of findings on the prone image through the lung bases (*E*), consistent with fibrosis. CPP are also visible on CT (*arrow*, *C*).

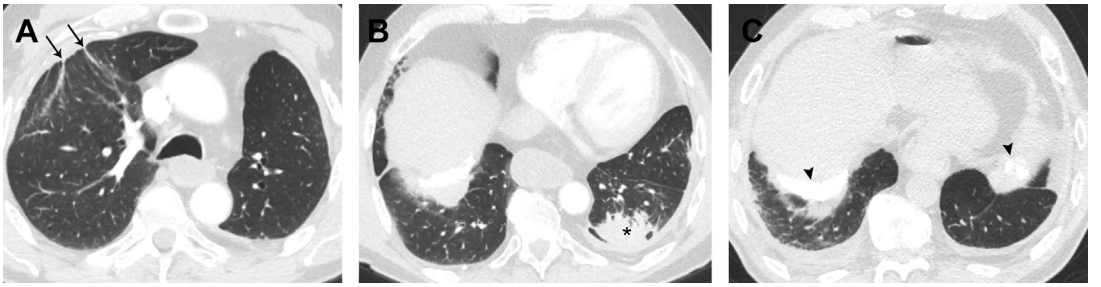

Fig. 5. Asbestos-related pleural and parenchymal changes. Axial CT image at the level of the carina (*A*) shows linear parenchymal bands coursing through right lung (*arrows*). Axial CT images through the lung bases (*B*, *C*) demonstrate a rounded atelectasis in the posterior left lower lobe (*, B). CPP are present along both hemidiaphragms (*arrowheads*, *C*). Note small bilateral pleural effusions and mild fibrosis in the right lung base (*C*).

asbestos-related pleural abnormalities are present in most individuals with asbestosis,[24] which can indicate an alternative diagnosis to IPF and suggest asbestosis.[26]

Rounded atelectasis is a round or oval opacity with volume loss adjacent to a pleural abnormality, often a pleural effusion, plaque, or thickening (**Fig. 5**). Rounded atelectasis is most common in the posterior lower lungs and can be diagnosed on CT if all of the following features are present: rounded or ovoid shape, volume loss, contact with the pleural surface, and vessels converging on the opacity with a curvilinear appearance (comet tail sign).[27] Uniform enhancement may be present after the administration of intravenous contrast material. If the appearance is atypical, FDG-PET/CT can be performed, which should not demonstrate increased FDG activity.[28]

SILICOSIS AND COAL WORKERS' PNEUMOCONIOSIS

Silicosis and CWP are 2 pathologically distinct entities occurring secondary to the inhalation of different inorganic dusts; however, the radiograph and HRCT appearances cannot be reliably distinguished.[3] Silicosis results from inhalation of crystalline silicone dioxide (silica). Occupations associated with silica exposure include tunneling, foundry work, sandblasting, mining, quarrying, drilling, stone cutting, polishing, brick lining, and ceramics manufacturing.[29] More recently, outbreaks of silicosis have been documented in association with engineered stone, a quartz based composite material.[30] CWP occurs in coal miners and is caused by the inhalation of coal dust free of silica. Both silicosis and CWP are risk factors for the development of tuberculosis and nontuberculous mycobacterial infections.[31,32]

There are 4 subtypes of silicosis: acute silicosis (silicoproteinosis), chronic simple silicosis, chronic complicated silicosis (progressive massive fibrosis [PMF]), and accelerated silicosis, depending on both the duration and intensity of the exposure, although more than one of these subtypes can coexist concurrently.[31]

Acute silicosis develops following acute exposure to very high concentrations of silica dust over months to several years, which results in filling of air spaces with proteinaceous material similar to idiopathic pulmonary alveolar proteinosis.[33] Radiograph findings include diffuse reticulonodular opacites and airspace consolidations, with or without air bronchograms, which may have a predilection for the upper lungs.[34] HRCT may show consolidations, greatest in the posterior lungs, and poorly defined soft tissue or ground glass centrilobular nodules. Foci of calcification are common, although are usually not seen in other entities presenting with acute consolidation, such as bacterial pneumonia or lymphoma.[33] Although a "crazy-paving" pattern of ground glass and superimposed septal thickening is associated with idiopathic pulmonary alveolar proteinosis, it is not typical for acute silicosis.[33]

Chronic simple silicosis and CWP typically develop 10 to 20 years after lower concentration exposure.[31] Radiographs demonstrate multiple solid, well-defined, small (<5 mm) pulmonary nodules that are most profuse in the upper posterior lung zones and may calcify.[6,35] HRCT appearance is most commonly small (<5 mm) bilateral pulmonary nodules with a predilection for the upper and posterior lung zones and either a centrilobular or perilymphatic distribution (**Fig. 6**).[35,36] Coalescence of subpleural nodules may result in pseudoplaques in both silicosis and CWP.[4] Pleural thickening has also been reported in both silicosis and CWP.[37,38] Mediastinal and hilar lymph node enlargement is often present and may demonstrate calcifications. Despite the commonly reported association with eggshell peripheral lymph node calcification, diffuse, punctate, and central patterns of calcification are actually more

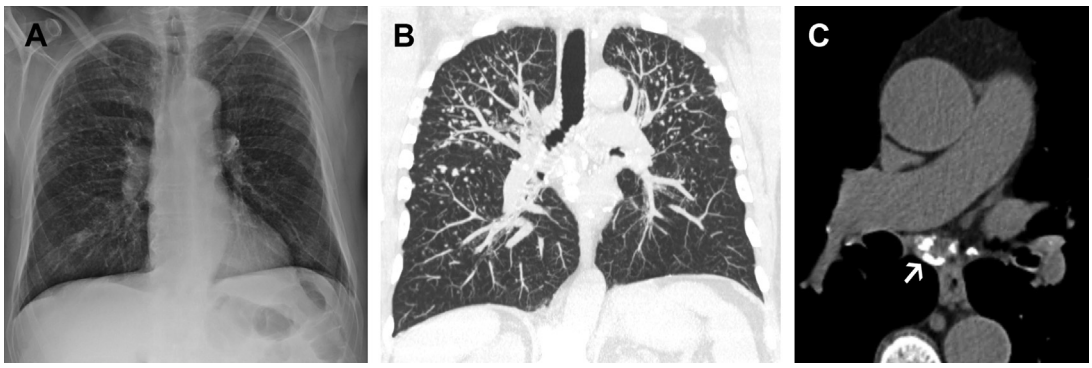

Fig. 6. Chronic simple silicosis. PA chest radiograph (*A*) and MIP coronal CT image (*B*) demonstrate numerous small, solid, perilymphatic distribution nodules with an upper lung predominance. Axial CT image (*C*) shows a mildly enlarged subcarinal lymph node with peripheral calcifications (*arrow*).

prevalent in silicosis. Eggshell calcifications are even less common in CWP.[36,39] Eggshell lymph node calcification can also be seen in chronic beryllium disease (CBD), sarcoidosis, amyloidosis, and some infections.[39]

Chronic complicated disease, or PMF, occurs more commonly with silicosis than CWP because silica is more fibrogenic than coal dust. PMF arises when small nodules coalesce into conglomerate nodules and masses that measure greater than 1 cm in diameter.[39] PMF can mimic the appearance of the conglomerate masses that form in advanced sarcoidosis.[6] In contrast to simple disease, PMF typically results in functional respiratory impairment.[6] The typical appearance of PMF on imaging is large bilateral opacities at the periphery of the upper lobes on a background of small nodules (**Figs. 7** and **8**). Paracicatricial emphysema may develop between the pleura and the opacities. Calcification is often present. Cavitation may occur due to ischemic necrosis or superimposed TB.[6,35] PMF may mimic lung cancer on imaging. MR imaging may be useful to help distinguish malignancy from PMF[40] but PET/CT has limited use because PMF may be FDG avid, even in the absence of superimposed malignancy or infection.[41] Biopsy or continued imaging surveillance may also be used in patients with PMF and concern for an underlying malignant mass.

Accelerated silicosis occurs with high-intensity exposure to silica dust, has shorter latency period of 4 to 10 years, and manifests similar to the complicated form of silicosis.[31,39]

CHRONIC BERYLLIUM DISEASE

Beryllium is a lightweight metal used in many industries including aerospace, ceramics, dentistry,

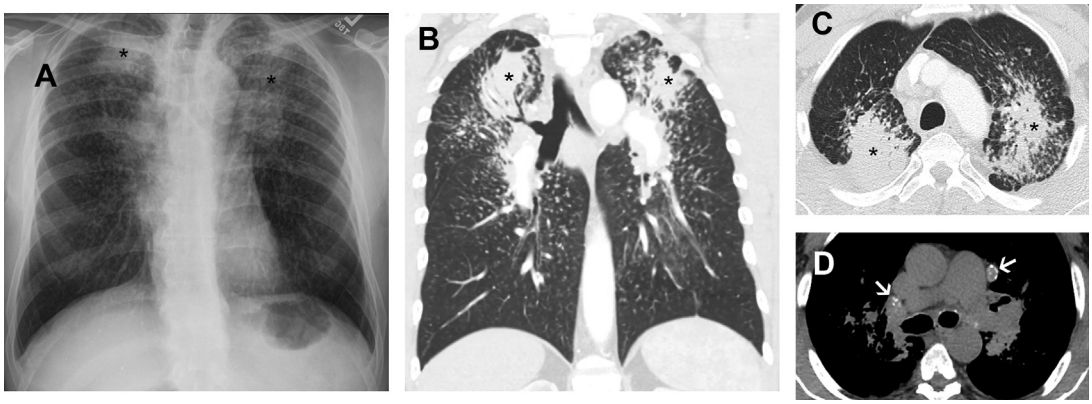

Fig. 7. Chronic complicated silicosis. PA chest radiograph (*A*) shows mass-like consolidation with volume loss in both upper lobes (*) on background of smaller upper lung predominant nodules. Coronal (*B*) and axial (*C*) chest CT images reveal innumerable small solid pulmonary nodules with an upper lung predominance and upper lung PMF (*). Axial CT soft tissue window image (*D*) demonstrates mildly enlarged lymph nodes with calcifications (*white arrows*).

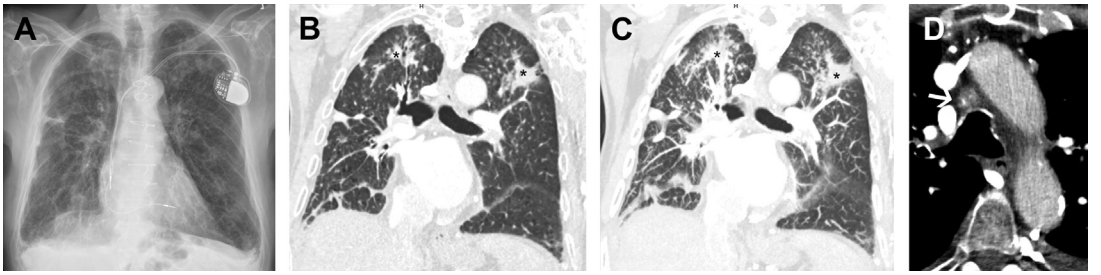

Fig. 8. Chronic complicated CWP. Frontal chest radiograph *(A)* shows ill-defined opacities in the bilateral upper lungs with associated volume loss and surrounding nodularity, as well as linear scarring and/or atelectasis in the mid and lower lungs. Thin section (*B*) and MIP (*C*) coronal CT images demonstrate PMF in both upper lobes (*) with surrounding small nodules. Axial CT image through the mediastinum (*D*) shows small calcifications in a paratracheal lymph node (*white arrow*).

nuclear, and electronics.[6] Acute berylliosis has been nearly eliminated in the United States due workplace regulations.[42] CBD occurs after exposure to beryllium or its salts, which may be in the form of dusts, fumes, or mists.[42] CBD is due to an immune-mediated delayed hypersensitivity response with the proliferation of beryllium-specific T cells.[43] CBD primarily affects the lungs; however, other organs may also be involved.[4] No clear dose–response relationship exists;CBD may occur after short-term, low-level exposure or may not develop even after long-term high-level exposure.[44] The diagnosis of CBD is based on exposure history, imaging, and the beryllium lymphocyte proliferation test. The beryllium lymphocyte proliferation test performed on blood or bronchiolar lavage fluid is quite sensitive and specific for CBD and useful in distinguishing CBD from mimics such as sarcoidosis.[42] As with silica and asbestos, beryllium exposure is thought to be a risk factor for developing lung carcinoma.[5]

Radiographs may appear normal in mild or early disease; however, patients with abnormal findings may have small irregular or round opacities, usually symmetric, and in either a mid-to-upper lung or diffuse distribution. Upper lung conglomerate masses, septal thickening, emphysema, upward hilar retraction with architectural distortion, linear scarring, hilar lymph node enlargement, and pleural thickening may also be observed.[42,45] HRCT findings include small nodules in a perilymphatic distribution, which are often associated with interlobular septal thickening. Additionally, conglomerate masses, GGOs, pleural abnormalities, bronchial wall thickening, and mediastinal and hilar lymphadenopathy may be seen (**Fig. 9**). Lymph nodes can calcify in an amorphous or eggshell pattern. As the disease progresses, fibrosis and occasionally honeycombing may occur.[35,46] In one study of a group of patients initially diagnosed with sarcoidosis, 40% were reclassified as having CBD after reevaluation.[47] Due to the overlap in imaging appearance, CBD should be considered when imaging findings are suggestive of sarcoidosis.

TALCOSIS

Talc is a hydrated magnesium silicate used in a variety of industries including rubber, plastics, textiles, and cosmetics.[4] The 3 forms of inhalational talc-related pulmonary diseases are pure talcosis, talcosilicosis, and talcoasbestosis. The fourth form of talcosis is due to the intravenous injection of crushed oral talc-containing medication tablets.[48] Talcosis produces a nonnecrotizing granulomatous reaction that may progress to fibrosis.[35] In the inhalational subtypes of talcosis, small diffuse rounded nodules are the most commonly described radiographic abnormality; however, larger nodular opacities greater than 1 cm and reticulations are also reported.[49] On HRCT, the most common finding is diffusely distributed centrilobular micronodules. Other findings include septal and subpleural lines, GGOs, large opacities with areas of high attenuation secondary to talc deposition, pleural plaques, and lymph node enlargement.[49,50] Talcoasbestosis and talcosilicosis often have imaging manifestations similar to asbestosis and silicosis, respectively.[48]

SIDEROSIS

Siderosis, also called “arc-welders’ pneumoconiosis,” is caused by the inhalation of inorganic welding smoke, which is primarily composed of iron oxide; however, several additional substances may also be present.[51] On chest radiograph, micronodules are sometimes visible.[51] The most common HRCT manifestation is defined pulmonary micronodules, often in a centrilobular

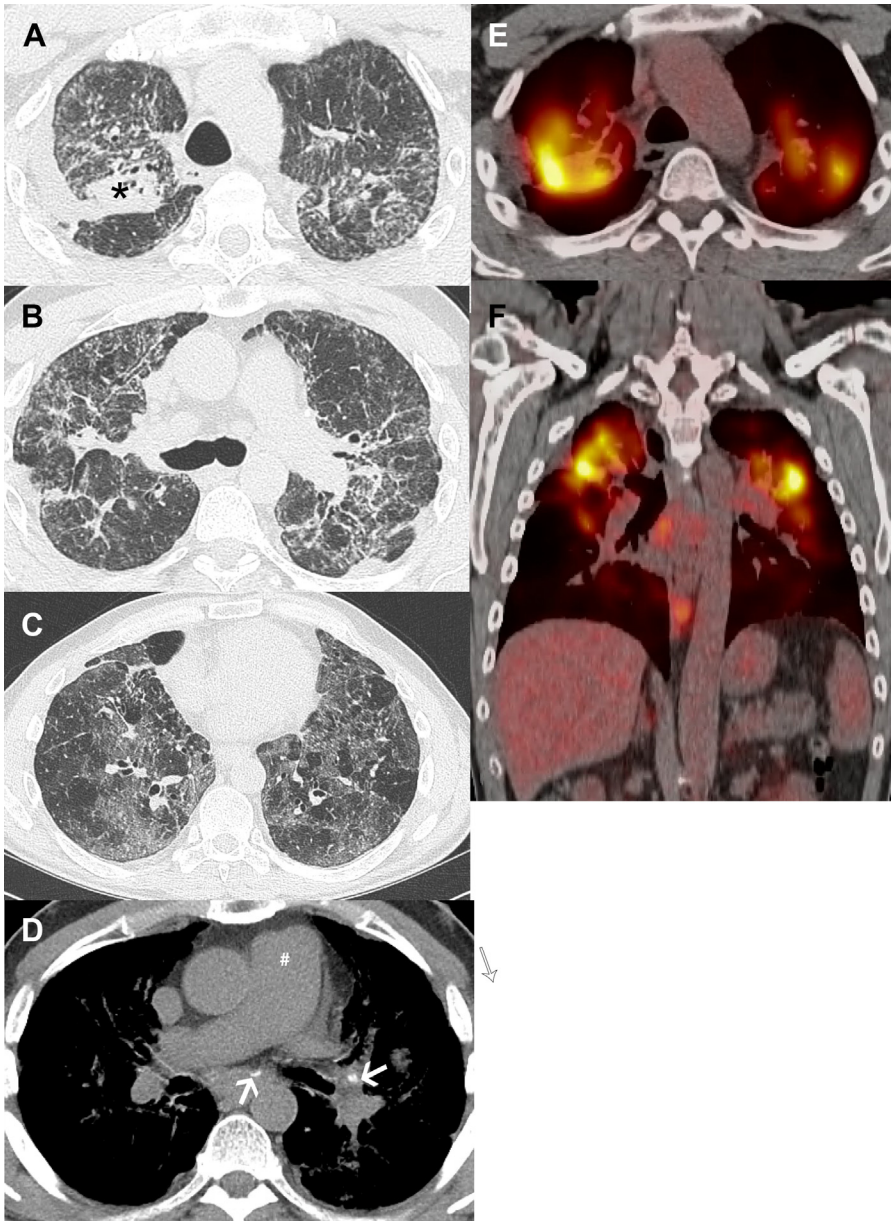

Fig. 9. CBD in a beryllium oxide machinist. Axial CT slices from the upper (*A*), mid (*B*), and lower (*C*) lungs demonstrate a conglomerate mass in the right upper lobe (*, A) with associated volume loss. Perihilar predominant perilymphatic nodularity, architectural distortion, interlobular septal thickening, and traction bronchiectasis are also present, greatest in the upper and mid lung zones. Diffuse GGOs and mosaic attenuation are present throughout the lungs but most conspicuous in the lung bases. Axial CT image on mediastinal window setting (*D*) reveals calcifications within hilar and subcarinal lymph nodes (*white arrows*). A dilated main pulmonary artery (#) is visible in the setting of known pulmonary hypertension. Axial (*E*) and coronal (*F*) FDG-PET/CT fusion images demonstrate increased FDG activity in the bilateral upper lungs associated with the conglomerate masses and more confluent regions of fibrosis.

distribution, reflecting accumulation of iron oxide particles in macrophages along peribronchiolar lymphatic vessels (**Fig. 10**).[51–53] Branching linear opacities have also been described and less commonly GGOs.[53] Ill-defined centrilobular micronodules and linear branching opacities are slightly more common in the upper lung zones, however relatively evenly distributed axially.[53] Findings can resemble hypersensitivity pneumonitis (HP), although mosaic attenuation may be a

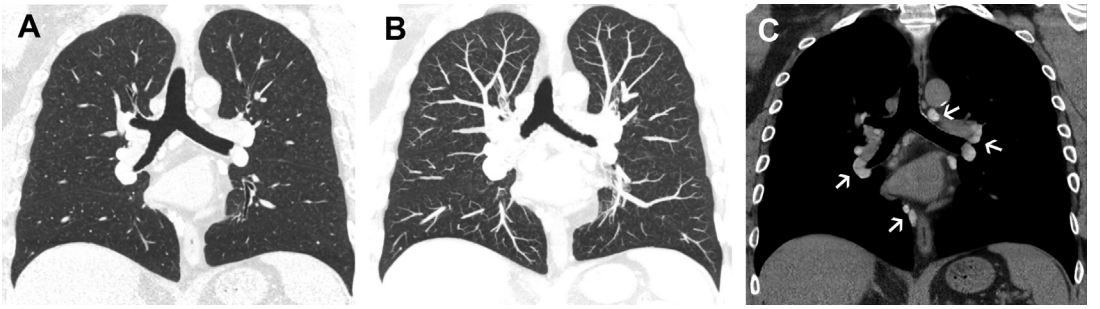

Fig. 10. Siderosis in a welder. Coronal CT thin section (*A*) and MIP (*B*) images demonstrate diffuse centrilobular micronodules throughout both lungs. Mediastinal window coronal CT image (*C*) shows numerous high attenuation mediastinal and bilateral hilar lymph nodes, some of which are enlarged.

more prominent feature in HP. Respiratory bronchiolitis and other infectious/inflammatory bronchiolitides are also on the differential.[43] Fibrosis is not a typical feature; however, it may result with additives to the welding process, such as silica.[53]

HARD METAL PNEUMOCONIOSIS

Hard metal pneumoconiosis (HMP) is caused by the inhalation of the dusts from alloys of tungsten, carbon, and cobalt, sometimes with the addition of small quantities of other metals; cobalt is the

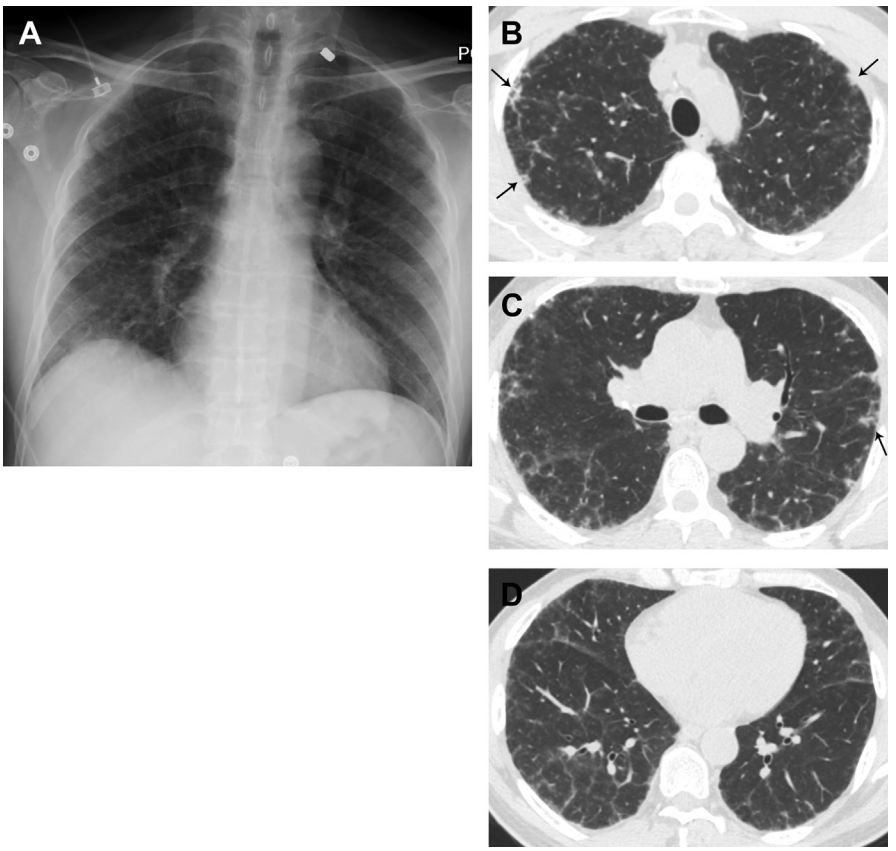

Fig. 11. Hard metal lung disease in a machinist working with tungsten carbide and cobalt-based alloys. Frontal chest radiograph (*A*) shows ill-defined bilateral linear and small nodular consolidative opacities in the periphery of both lungs. Axial chest CT images through the upper (*B*), mid (*C*), and lower (*D*) lungs show peripheral reticular opacities with mild architectural distortion and small areas of mildly nodular consolidation (*arrows*, *B*, *C*). Subtle ill-defined GGOs and interlobular septal thickening are also present (*C*, *D*).

primary component implicated in the pulmonary toxicity.[3,4] These durable and heat-resistant alloys are used in polishing, drilling, grinding, and cutting metals or other hard materials due to their durability and heat-resistant properties. Exposure can result in interstitial pneumonitis and fibrosis.[3] On histopathology, HMP can take several forms; however, giant cell interstitial pneumonia is nearly pathognomonic, when present.[54] Chest radiograph appearance is nonspecific and may be normal, show small nodules and reticular opacities, or fibrosis.[35] HRCT findings include consolidative opacities, which may contain air bronchograms and traction bronchiectasis, and multilobular or panlobular GGOs (**Fig. 11**).[52] Reticulation, subpleural cystic spaces, and nodular peribronchovascular thickening with traction bronchiectasis have also been reported.[55] Thus, HMP can appear similar to sarcoidosis, NSIP, and/or UIP on imaging.[55] The diagnosis of HMP requires a combination of exposure history, clinical symptoms, radiologic findings of interstitial lung disease, and histologic findings of interstitial lung disease or giant cell pneumonia, as well as histopathologic findings of metal in lung tissue.[35]

ALUMINOSIS

Aluminosis is caused by the inhalation of aluminum powder and aluminum oxide[56] with exposures including alumina abrasive manufacture and pyrotechnic manufacture.[57] In early disease, radiographs may be unrevealing or demonstrate upper or mid lung predominant small rounded and irregular opacities. In later disease, upper lung fibrotic changes may be visible.[31,56] HRCT findings of early aluminosis include small rounded ill-defined centrilobular opacities measuring 3 mm or less with an upper lung predominance. This pattern may resemble HP, silicosis, CWP, or respiratory bronchiolitis.[31,56] In advanced disease, HRCT may demonstrate upper lung predominant reticular and nodular interstitial fibrosis with subpleural emphysema, mimicking silicosis, CWP, sarcoidosis, or HP.[31,56] Increased attenuation within mediastinal and hilar lymph nodes due to aluminum deposition has been reported.[58]

HYPERSENSITIVITY PNEUMONITIS

HP is an immunologically mediated process caused by the inhalation of organic antigens, which can occur due to occupational or

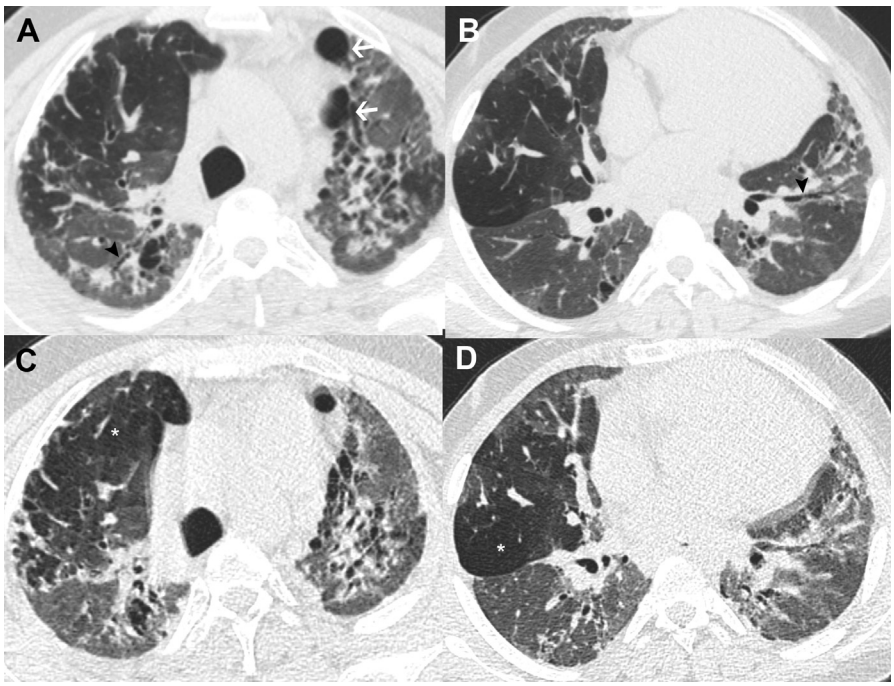

Fig. 12. Subacute on chronic HP in an individual with substantial exposure to chickens and positive avian antigens. Axial inspiratory CT images through the mid and lower lungs (*A*, *B*) with expiratory CT images at corresponding locations (C, D, respectively) demonstrate mosaic attenuation of the lung parenchyma with areas of air trapping (*, C, D). Peripheral and peribronchovascular distribution irregular opacities with architectural distortion, volume loss, and traction bronchiectasis (*arrowheads*, *A*, *B*) are also present, consistent with fibrosis. Subpleural cysts are also present (*arrow*, *A*).

nonoccupational exposures. HP develops in susceptible individuals following sensitization and subsequent repeated exposure to a variety of organic antigens, including those from animals, plants, bacteria, fungi, and some chemicals. HP subtypes are often named to reflect the causative agent, for example, "bird fancier's lung" and "farmer's lung." The most common inciting antigens in a study from the United States were avian antigens, followed by hot tub-related *Mycobacterium avium* complex; however, no specific antigen was identified in one-quarter of cases.[59] A diagnosis of HP considers clinical, imaging, laboratory, and sometimes histopathologic data.[60] HP has historically been characterized as either acute, subacute, or chronic; however, classification into fibrotic versus nonfibrotic subtypes is now preferred.[60]

Consistent imaging findings in acute HP are less well reported but airspace consolidations may be seen.[3]

HRCT findings of subacute HP include patchy or diffuse ground-glass opacities and small (<5 mm) poorly defined centrilobular nodules, which may be uniformly distributed or be more pronounced in the mid to lower lungs. Inspiratory images demonstrate mosaic attenuation corresponding with air trapping on expiratory images.[61] The head-cheese sign, named for its resemblance to the processed meat product, has been described in subacute HP and reflects a patchwork of different lung attenuations: hyperlucent lung caused by air trapping, GGOs due to interstitial pneumonitis, and regions of normal lung attenuation.[62]

Chronic HP is characterized by fibrosis visible as reticulations, ground glass, volume loss, and traction bronchiectasis in patchy, subpleural, or peribronchovascular distribution (**Fig. 12**). Fibrosis may have an upper or lower lung predominance or no zonal predilection; however, the costophrenic sulci and apices may be spared.[63] Subpleural honeycombing is a marker of advanced disease and more often upper lobe predominant; this is in contrast to IPF characterized by basilar predominant honeycombing.[63] Air trapping on expiratory images is common, which may be helpful in distinguishing HP from IPF or NSIP.[63,64] Cysts are also substantially more prevalent in HP than in IPF or NSIP.[63] Studies also have demonstrated high rates of emphysema in nonsmoking farmers and bird fanciers with chronic HP.[65,66]

WORK-RELATED ASTHMA

Work-related asthma is the most common form of OLD and includes both work-exacerbated asthma (preexisting asthma worsened by workplace exposures) and occupational asthma (asthma caused by airborne dusts, vapors gases, or fumes in the workplace).[6] Imaging findings cannot be differentiated from nonoccupational causes of small airways disease. On radiographs, pulmonary hyperinflation and bronchial wall thickening may be visible. HRCT findings are those of small airways disease including mosaic attenuation, bronchial wall thickening, and air trapping on expiratory images.[6]

SUMMARY

Despite regulations, OLDs remain a leading cause of work-related illnesses. Establishing a diagnosis of an OLD often requires a multidisciplinary approach, incorporating a thorough exposure of history and other diagnostic data, including imaging. Although radiographs remain the standard for screening and surveillance, HRCT is often both more sensitive and specific for evaluation. Substantial overlap in imaging findings exists between many OLDs and other entities including fibrotic interstitial lung diseases, sarcoidosis, and infectious processes. As a result, the radiologist should be familiar with the myriad of imaging appearances and consider OLDs when formulating a differential.

CLINICS CARE POINTS

- Because substantial overlap exists between the imaging appearances of OLDs and other nonoccupational entities, OLDs should be considered when formulating a differential.
- Establishing the diagnosis of an OLD often requires a multidisciplinary approach and integration of a thorough exposure history, laboratory results, diagnostic imaging, pulmonary function testing, and sometimes biopsy.
- HRCT is often both more sensitive and specific for the evaluation of OLDs than radiographs.

DISCLOSURE

The authors have nothing to disclose.

REFERENCES

1. Vlahovich KP, Sood AA. 2019 Update on Occupational Lung Diseases: A Narrative Review. Pulm Ther 2021;7(1):75–87.

2. Weston A. Work-related lung diseases. IARC Sci Publ 2011;163:387–405.
3. Kim KI, Kim CW, Lee MK, et al. Imaging of occupational lung disease. Radiographics 2001;21(6):1371–91.
4. Ahuja J, Kanne JP, Meyer CA. Occupational lung disease. Semin Roentgenol 2015;50(1):40–51.
5. Cox CW, Rose CS, Lynch DA. State of the art: Imaging of occupational lung disease. Radiology 2014; 270(3):681–96.
6. Champlin J, Edwards R, Pipavath S. Imaging of Occupational Lung Disease. Radiol Clin North Am 2016;54(6):1077–96.
7. Remy-Jardin M, Degreef JM, Beuscart R, et al. Coal worker's pneumoconiosis: CT assessment in exposed workers and correlation with radiographic findings. Radiology 1990;177(2):363–71.
8. Gevenois PA, Pichot E, Dargent F, et al. Low grade coal worker's pneumoconiosis. Comparison of CT and chest radiography. Acta Radiol 1994;35(4): 351–6.
9. al Jarad N, Poulakis N, Pearson MC, et al. Assessment of asbestos-induced pleural disease by computed tomography–correlation with chest radiograph and lung function. Respir Med 1991;85(3):203–8.
10. Aberle DR, Gamsu G, Ray CS. High-resolution CT of benign asbestos-related diseases: clinical and radiographic correlation. AJR Am J Roentgenol 1988;151(5):883–91.
11. Guidelines for the use of the ILO International classification of radiographs of pneumoconioses. Geneva: International Labour Office; 2011. p. 2011. Available at: https://www.ilo.org/wcmsp5/groups/public/—ed_protect/—protrav/—safework/documents/publication/wcms_168260.pdf.
12. Mossman BT, Churg A. Mechanisms in the pathogenesis of asbestosis and silicosis. Am J Respir Crit Care Med 1998;157(5 Pt 1):1666–80.
13. Peacock C, Copley SJ, Hansell DM. Asbestos-related benign pleural disease. Clin Radiol 2000; 55(6):422–32.
14. Epler GR, McLoud TC, Gaensler EA. Prevalence and incidence of benign asbestos pleural effusion in a working population. JAMA 1982;247(5):617–22.
15. Hillerdal G, Ozesmi M. Benign asbestos pleural effusion: 73 exudates in 60 patients. Eur J Respir Dis 1987;71(2):113–21.
16. Lynch DA, Gamsu G, Aberle DR. Conventional and high resolution computed tomography in the diagnosis of asbestos-related diseases. Radiographics 1989;9(3):523–51.
17. Fletcher DE, Edge JR. The early radiological changes in pulmonary and pleural asbestosis. Clin Radiol 1970;21(4):355–65.
18. McLoud TC, Woods BO, Carrington CB, et al. Diffuse pleural thickening in an asbestos-exposed population: prevalence and causes. AJR Am J Roentgenol 1985;144(1):9–18.
19. Hobbs SB. Asbestos-Related Disease. In: Walker CM, Chung JH, Hobbs SB, et al, editors. Müller's imaging of the chest. 2nd edition. Philadelphia, PA: Elsevier Health Sciences; 2019. p. 775–92.
20. Cugell DW, Kamp DW. Asbestos and the pleura: a review. Chest 2004;125(3):1103–17.
21. Yates DH, Corrin B, Stidolph PN, et al. Malignant mesothelioma in south east England: clinicopathological experience of 272 cases. Thorax 1997;52(6):507–12.
22. Leung AN, Muller NL, Miller RR. CT in differential diagnosis of diffuse pleural disease. AJR Am J Roentgenol 1990;154(3):487–92.
23. Akira M, Yokoyama K, Yamamoto S, et al. Early asbestosis: evaluation with high-resolution CT. Radiology 1991;178(2):409–16.
24. Aberle DR, Gamsu G, Ray CS, et al. Asbestos-related pleural and parenchymal fibrosis: detection with high-resolution CT. Radiology 1988;166(3): 729–34.
25. al-Jarad N, Strickland B, Pearson MC, et al. High resolution computed tomographic assessment of asbestosis and cryptogenic fibrosing alveolitis: a comparative study. Thorax 1992;47(8):645–50.
26. Raghu G, Remy-Jardin M, Myers JL, et al. Diagnosis of Idiopathic Pulmonary Fibrosis. An Official ATS/ERS/JRS/ALAT Clinical Practice Guideline. Am J Respir Crit Care Med 2018;198(5):e44–68.
27. Batra P, Brown K, Hayashi K, et al. Rounded atelectasis. J Thorac Imaging 1996;11(3):187–97.
28. McAdams HP, Erasums JJ, Patz EF, et al. Evaluation of patients with round atelectasis using 2-[18F]-fluoro-2-deoxy-D-glucose PET. J Comput Assist Tomogr 1998;22(4):601–4.
29. Bang KM, Attfield MD, Wood JM, et al. National trends in silicosis mortality in the United States, 1981-2004. Am J Ind Med 2008;51(9):633–9.
30. Rose C, Heinzerling A, Patel K, et al. Severe Silicosis in Engineered Stone Fabrication Workers - California, Colorado, Texas, and Washington, 2017-2019. MMWR Morb Mortal Wkly Rep 2019;68(38):813–8.
31. Hobbs SB. Silicosis and Coal Workers' Pneumoconiosis. In: Walker C, Chung J, Hobbs S, et al, editors. Müller's imaging of the chest. 2nd edition. Philadelphia, PA: Elsevier Health Sciences; 2019. p. 793–808.
32. Cowie RL. The epidemiology of tuberculosis in gold miners with silicosis. Am J Respir Crit Care Med 1994;150(5 Pt 1):1460–2.
33. Marchiori E, Souza CA, Barbassa TG, et al. Silicoproteinosis: high-resolution CT findings in 13 patients. AJR Am J Roentgenol 2007;189(6):1402–6.
34. Dee P, Suratt P, Winn W. The radiographic findings in acute silicosis. Radiology 1978;126(2):359–63.
35. Chong S, Lee KS, Chung MJ, et al. Pneumoconiosis: comparison of imaging and pathologic findings. Radiographics 2006;26(1):59–77.

36. Antao VC, Pinheiro GA, Terra-Filho M, et al. High-resolution CT in silicosis: correlation with radiographic findings and functional impairment. J Comput Assist Tomogr 2005;29(3):350–6.
37. Young RC Jr, Rachal RE, Carr PG, et al. Patterns of coal workers' pneumoconiosis in Appalachian former coal miners. J Natl Med Assoc 1992;84(1):41–8.
38. Arakawa H, Honma K, Saito Y, et al. Pleural disease in silicosis: pleural thickening, effusion, and invagination. Radiology 2005;236(2):685–93.
39. Batra K, Aziz MU, Adams TN, et al. Imaging Of Occupational Lung Diseases. Semin Roentgenol 2019;54(1):44–58.
40. Ogihara Y, Ashizawa K, Hayashi H, et al. Progressive massive fibrosis in patients with pneumoconiosis: utility of MRI in differentiating from lung cancer. Acta Radiol 2018;59(1):72–80.
41. Chung SY, Lee JH, Kim TH, et al. 18F-FDG PET imaging of progressive massive fibrosis. Ann Nucl Med 2010;24(1):21–7.
42. Aronchick JM, Rossman MD, Miller WT. Chronic beryllium disease: diagnosis, radiographic findings, and correlation with pulmonary function tests. Radiology 1987;163(3):677–82.
43. Hobbs SB, Uncommon Pneumoconioses. In: Walker CM, Chung JH, Hobbs SB, et al., Eds Müller's Imaging of the Chest. 2nd ed. Elsevier Philadelphia, PA; 2019:809-821.
44. Kreiss K, Mroz MM, Zhen B, et al. Epidemiology of beryllium sensitization and disease in nuclear workers. Am Rev Respir Dis 1993;148(4 Pt 1): 985–91.
45. Sharma N, Patel J, Mohammed TL. Chronic beryllium disease: computed tomographic findings. J Comput Assist Tomogr 2010;34(6):945–8.
46. Newman LS, Buschman DL, Newell JD Jr, et al. Beryllium disease: assessment with CT. Radiology 1994;190(3):835–40.
47. Muller-Quernheim J, Gaede KI, Fireman E, et al. Diagnoses of chronic beryllium disease within cohorts of sarcoidosis patients. Eur Respir J 2006;27(6): 1190–5.
48. Feigin DS. Talc: understanding its manifestations in the chest. AJR Am J Roentgenol 1986;146(2): 295–301.
49. Akira M, Kozuka T, Yamamoto S, et al. Inhalational talc pneumoconiosis: radiographic and CT findings in 14 patients. AJR Am J Roentgenol 2007;188(2): 326–33.
50. Marchiori E, Souza Junior AS, Muller NL. Inhalational pulmonary talcosis: high-resolution CT findings in 3 patients. J Thorac Imaging 2004;19(1):41–4.
51. Takahashi M, Nitta N, Kishimoto T, et al. Computed tomography findings of arc-welders' pneumoconiosis: Comparison with silicosis. Eur J Radiol 2018; 107:98–104.
52. Akira M. Uncommon pneumoconioses: CT and pathologic findings. Radiology 1995;197(2):403–9.
53. Han D, Goo JM, Im JG, et al. Thin-section CT findings of arc-welders' pneumoconiosis. Korean J Radiol 2000;1(2):79–83.
54. Ohori NP, Sciurba FC, Owens GR, et al. Giant-cell interstitial pneumonia and hard-metal pneumoconiosis. A clinicopathologic study of four cases and review of the literature. Am J Surg Pathol 1989;13(7): 581–7.
55. Gotway MB, Golden JA, Warnock M, et al. Hard metal interstitial lung disease: high-resolution computed tomography appearance. J Thorac Imaging 2002;17(4):314–8.
56. Kraus T, Schaller KH, Angerer J, et al. Aluminosis–detection of an almost forgotten disease with HRCT. J Occup Med Toxicol 2006;1:4.
57. Guidotti T. Pulmonary aluminosis-a review. Toxicol Pathol 1975;3:16–8.
58. Vahlensieck M, Overlack A, Muller KM. Computed tomographic high-attenuation mediastinal lymph nodes after aluminum exposition. Eur Radiol 2000; 10(12):1945–6.
59. Hanak V, Golbin JM, Ryu JH. Causes and presenting features in 85 consecutive patients with hypersensitivity pneumonitis. Mayo Clin Proc 2007;82(7):812–6.
60. Raghu G, Remy-Jardin M, Ryerson CJ, et al. Diagnosis of Hypersensitivity Pneumonitis in Adults. An Official ATS/JRS/ALAT Clinical Practice Guideline. Am J Respir Crit Care Med 2020;202(3):e36–69.
61. Glazer CS, Rose CS, Lynch DA. Clinical and radiologic manifestations of hypersensitivity pneumonitis. J Thorac Imaging 2002;17(4):261–72.
62. Torres PP, Moreira MA, Silva DG, et al. High-resolution computed tomography and histopathological findings in hypersensitivity pneumonitis: a pictorial essay. Radiol Bras 2016;49(2):112–6.
63. Silva CI, Muller NL, Lynch DA, et al. Chronic hypersensitivity pneumonitis: differentiation from idiopathic pulmonary fibrosis and nonspecific interstitial pneumonia by using thin-section CT. Radiology 2008;246(1):288–97.
64. Silva CI, Churg A, Muller NL. Hypersensitivity pneumonitis: spectrum of high-resolution CT and pathologic findings. AJR Am J Roentgenol 2007;188(2): 334–44.
65. Remy-Jardin M, Remy J, Wallaert B, et al. Subacute and chronic bird breeder hypersensitivity pneumonitis: sequential evaluation with CT and correlation with lung function tests and bronchoalveolar lavage. Radiology 1993;189(1):111–8.
66. Erkinjuntti-Pekkanen R, Rytkonen H, Kokkarinen JI, et al. Long-term risk of emphysema in patients with farmer's lung and matched control farmers. Am J Respir Crit Care Med 1998;158(2):662–5.